An Overview of Rapidly Prototyped Piezoelectric Actuators and Grain-Oriented Ceramics

M. ALLAHVERDI, A. HALL, R. BRENNAN, M.E. EBRAHIMI, N. MARANDIAN HAGH & A. SAFARI*

Department of Ceramic and Materials Engineering, Rutgers, The State University of New Jersey, 607 Taylor Road, Piscataway, NJ 08854, USA

Abstract. Rapid prototyping (RP) has been used to fabricate a series of piezoelectric actuators, including spiral and tube actuators, to study the actuation mechanism in these geometries, and to obtain enhanced properties. PZT spiral actuators showed large displacement in mm range, and moderate blocking force. Unimorph spirals (PZT/metal shim) and dual-material (piezoelectric/electrostrictive) PMN-PT spirals were also prototyped and characterized. Tube actuators with inward and outward wall curvature showed slight improvement in axial and radial displacements compared to conventional straight-walled tube actuators. In order to improve the performance of ceramic actuators with polycrystalline microstructures, grain-oriented ceramics of bismuth titanate, lead metaniobate, and PMN-PT were investigated. Texturing was achieved by incorporating anisometric seeds into RP feedstock, aligning them during fabrication, and growing the seeds (templates) at elevated temperatures. Synthesis of anisometric seeds and pertinent processing conditions of the textured ceramics are presented. The feasibility of making net shape single crystal components was also explored. Single crystals of 0.65PMN-0.35PT were grown in FDC components using embedded (111) and (110) $SrTiO_3$ seeds at 1250°C.

Keywords: rapid prototyping, actuators, piezoelectric, grain orientation, single crystal

Introduction

Several piezoelectric actuators with novel designs have been made and characterized in the last few years [1–3]. It has been demonstrated that improved electromechanical properties can be achieved by tailoring the geometry and dimensions of an actuator. Ceramic processing techniques, such as injection molding, are too costly and time-consuming to develop and prototype new actuators. The recent implementation of Rapid Prototyping (RP) to build intricate components directly from CAD files has brought a high degree of flexibility, cost-effectiveness and speed to the field of piezoelectric applications.

In the last seven years, RP methods of Fused Deposition of Ceramics (FDC) have been utilized to fabricate a series of piezoelectric actuators [2, 4–9]. This article briefly reviews the processing and properties of rapidly prototyped actuators, empha-

sizing the recent results on unimorph and bimaterial spirals, as well as tube actuators with curved tube walls. Prototyped ceramics of lead metaniobate and PMN-PT with grain-oriented microstructures and pseudo-single crystals are also presented.

Prototyped Piezoelectric Actuators

Piezoelectric actuators generate field-induced displacements that can be used in motion systems such as micro-positioners, ultrasonic motors, and vibration damping. It is desirable to enhance the displacement while maintaining a reasonable amount of load bearing capability. This has been achieved by manipulating the geometry of simple shape (rod or strip) actuators into more complex geometries [1, 2, 10, 11]. For example, the axial displacement of a solid piezoelectric cylinder (rod) can be improved by replacing it with a tube actuator. Other techniques such as addition of a stiff inactive layer (a metal shim in unimorph and

---

*To whom all correspondence should be addressed.

bimorph actuators) have also been utilized to improve displacement [3, 12].

Using the RP technique of FDC, a series of novel actuators has been designed and prototyped to study the effect of design/geometry on the field-induced displacement. The flexibility of FDC has allowed for the rapid fabrication of actuators with complex geometry that cannot easily be made by conventional manufacturing techniques. These actuators include spiral [2], telescoping [8], dome [9], tube [13], curved and multi-layered tubes, bellows, and bimorph benders [7]. Spiral and tube actuators will be briefly reviewed with emphasis on the recent results.

Spiral Actuators

In order to enlarge field-induced displacement, spiral actuators with a compact geometry were designed and prototyped (Fig. 1(a)). The application of an electric field across the spiral width induces both tangential and radial displacements, the former being much larger than the latter. It has been shown that for a PZT spiral actuator with 32 mm diameter, the tangential movement
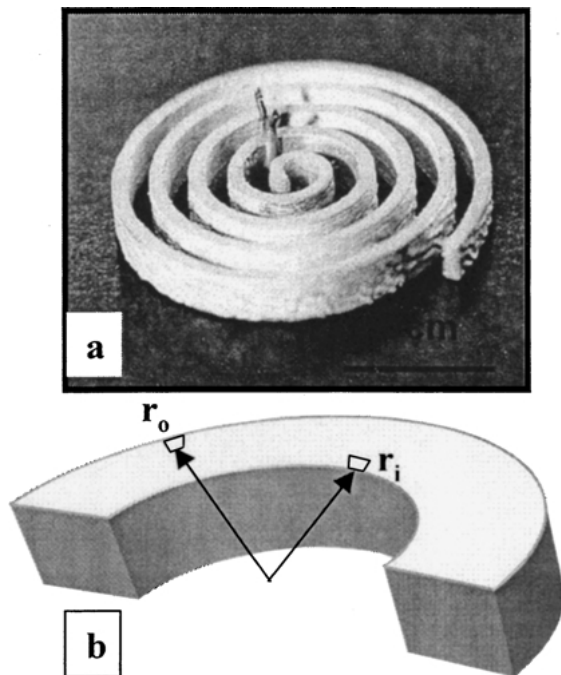

Fig. 1. (a) Spiral actuator and (b) schematic of a curved piezoelectric segment, illustrating elements in the outer and inner diameters. A slight displacement gradient exists across the thickness, resulting in bending stress and segment rotation.

reaches 1.9 mm at ~11.6 kV/cm [8]. This is about twelve times higher than the displacement of a PZT strip of the same dimensions, which clearly shows that displacement can profoundly be enhanced by tailoring the geometry of the actuator.

In a curved geometry like a spiral, there exists a slight gradient in the displacement of small elements across the thickness (Fig. 1(b)). This means that the displacement of an element in the outer diameter (r_o) is larger than that of an element in the inner diameter (r_i). Such a phenomenon creates a bending moment, which leads to rotation and/or large tangential displacement in spirals. The large actuation of spirals is obtained at the cost of load bearing capability since the two are inversely related. For example, the blocking force for the above-mentioned spiral actuator, measured at various electric fields (1.3 to 3.3 kV/cm), is ~0.8 N [8]. Despite low blocking force, spiral actuators are of interest due to large displacement and compact geometry.

To further enhance the actuation, unimorph PZT spiral actuators have been investigated. Modeling results of spirals have suggested that asymmetric electrodes/shims can enhance the tangential displacement significantly [14]. Unimorph spirals were fabricated by attaching a stainless steel shim on the inner side of the spiral wall. In a conventional unimorph, the relative difference between the length of ceramic and metal strips under an electric field results in bending, and therefore, large tip displacement. A PZT spiral actuator (width = 1.05 mm, diameter = 28.85 mm, height = 2.55 mm) with a 37.5 μm stainless steel shim was fabricated and tested. The addition of the stainless steel shim increased the tangential displacement by 200% at 850 V, as depicted in Fig. 2. This
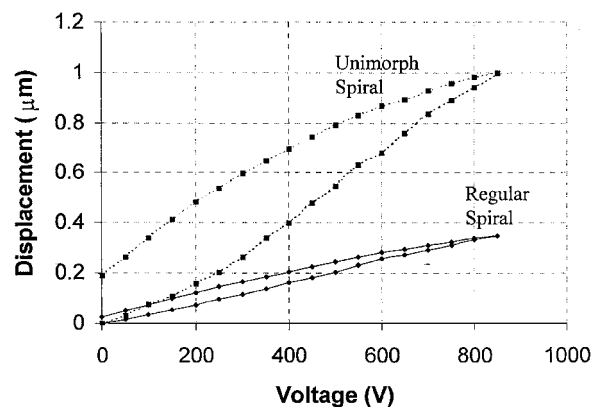

Fig. 2. Displacement enhancement in PZT spiral actuator as a result of adding a 37.5 μm shim.

increase in displacement is analogous to the bending of a conventional unimorph. It is also seen that the hysteresis of the unimorph spiral was much higher (e.g., about six times higher at 400 V) than the regular spiral actuator. Experiments are currently under progress to determine the effect of shim thickness on tangential displacement.

In another series of experiments, the tangential displacement of spirals with dissimilar ceramic strips was investigated. For this purpose, bimaterial spiral actuators consisting of one piezoelectric and one electrostrictive PMN-PT layer with the same thickness were fabricated and tested. These actuators can be driven in such a way that the piezoelectric spiral expands tangentially whereas the electrostrictive layer contracts. This would further enhance the bending moment of the spiral. The bimaterial spiral actuator was designed such that the outer side of the spiral wall was the piezoelectric 0.65PMN-0.35PT layer while the inner side of the wall was the electrostrictive 0.90PMN-0.10PT layer. Such spirals were prototyped by FDC and cofired successfully at 1250°C for 1 hr. Measurements have shown that the piezoelectric/electrostrictive (PE) spiral actuator has yielded higher displacements than a PZT actuator (Fig. 3) of similar dimensions. For example, the PE actuator displaced to ∼510 μm at 500V as compared to ∼200 μm for the PZT actuator at the same DC biased field. The enhancement of tangential displacement was accompanied by large hysteresis of the PE actuators similar to the unimorph spirals.
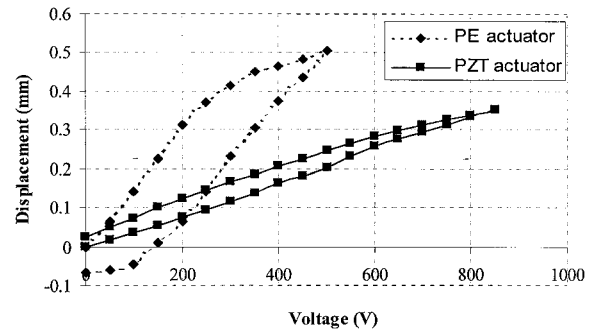

Fig. 3. A comparison of the tangential displacements of the PZT and Piezoelectric/Electrostrictive PMN-PT actuators under DC biased voltage.

Tube Actuators

Piezoelectric tubes are utilized for actuator (Ink Jet Printing) and sensor (1-3 piezocomposites) applications [15, 16]. Tube actuators have demonstrated promising properties and been successfully used to shift mirrors of laser resonators in scanning tunnel microscopy and atomic force microscopes.

Single tube and tube arrays (Fig. 4(a)) were fabricated with various diameter, height, and wall thickness via the FDC process [13]. Tube geometry has been modified to tune properties (e.g., resonance frequency and axial displacement) for a given application. Tube actuators with zigzag wall design (bellows, Fig. 4(b)) have also been prototyped to study the effect of wall configuration (bellows angle) on the axial and radial
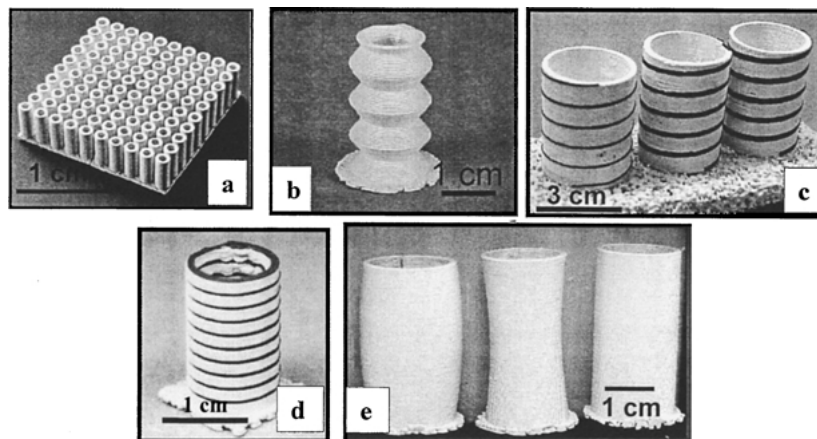

Fig. 4. Various tube actuators made by the FDC process. (a) tube array, (b) bellows, (c) tubes with helical electrodes, (d) multilayer tube, and (e) tubes with curved walls.

displacements [17]. Comparison of bellows with the straight tubes revealed that the bellows possess up to 50% larger radial displacements, whereas their axial displacements were about 20–30% lower.

Another type of tube actuator with helical electrodes has also been investigated (Fig. 4(c)). Normally, the inner and outer surfaces of the tubes are electroded and poled radially. In this manner, the actuation or sensing is based on the d_{31} coefficient. However, in the new design the electrodes are laid side by side in helical form along the tube height [18]. For such piezoelectric tubes, displacement is derived from the d_{33} coefficient, resulting in an improvement of more than two times in axial displacement ($d_{33}/d_{31} > 2$). In addition to tubes with helical electrodes, multilayer tube actuators (Fig. 4(d)) also benefit from the larger piezoelectric coefficient of d_{33}. Successful fabrication of these actuators depends upon the electrode materials, its thickness, and sintering conditions/atmosphere [18].

It has been shown that the actuation of a piezoelectric element can be improved if a given structure is curved. For example, dome [9], RAINBOW (Reduced and Internally Biased Oxide Wafer [1]), and THUNDER (Thin Layer Unimorph Driver [10]) actuators illustrate displacement enhancement as a result of curved geometry. In order to determine if curvature would have a positive impact on tube actuators, PZT tubes with curved walls (both inward and outward curvatures (Fig. 4(e)) were designed, prototyped, and characterized. All the green tubes were of the same height, end diameter and wall thickness (20 mm, 15 mm, and 1 mm, respectively). The axial and radial displacements of these tubes, measured by a photonic sensor, are plotted in Fig. 5. Despite the large variation of data points, it appears that the regular (straight-walled or radial ratio of 1) tubes showed minimum displacement whereas the curved-wall tubes showed slightly larger actuations, likely due to the wall curvature. It is speculated that the constrained geometry of these actuators (tubular shape) limits the contribution of the curvature, and therefore, only slight improvement can be gained in radial and axial displacements.

Prototyped Components with Oriented Microstructures

The piezoelectric properties of ferroelectric crystals are normally anisotropic, illustrating superior properties in certain directions. However, in polycrystalline ferroelectrics, grain orientation is random, and therefore, the anisotropy is lost. Poling of random polycrystalline ceramics could be of poor quality due to low crystal symmetry that inhibits the appropriate orientation of the polarization axes [19]. Therefore, it is desirable to texture the piezoelectric ceramics to gain more efficient poling and enhanced properties. To generate grain-oriented microstructures, a novel technique, referred to as templated grain growth (TGG) [20–22], has been implemented to a variety of ceramics including piezoelectric and electrostrictive materials.

In the TGG process, small templates (seeds) are initially oriented in a polycrystalline matrix. A grain-oriented microstructure, with a majority of the grains aligned in a certain direction may form upon suitable heat treatment. In order to achieve primary orientation, a small percentage of anisometric (i.e., needle or platelet) templates is primarily oriented within the fine polycrystalline matrix using a shear forming technique such as tape casting. It is crucial to have high aspect ratio templates and proper alignment in order to develop microstructures with highly oriented grains.

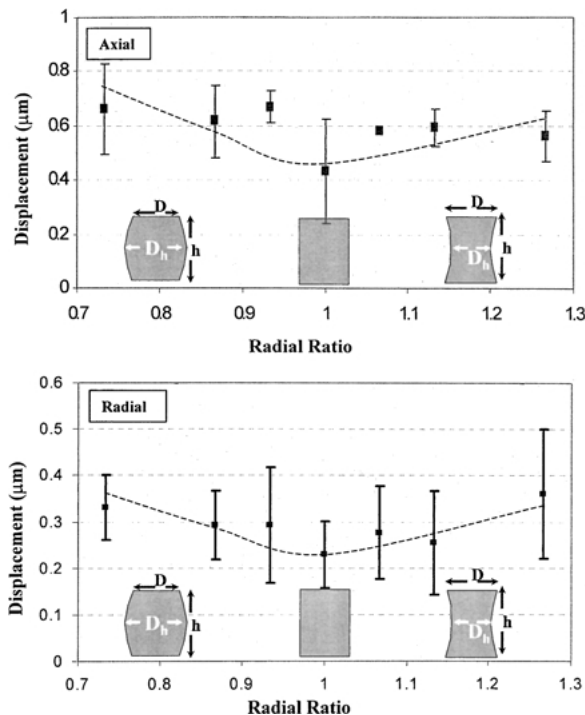We have explored the feasibility of fabricating grain-oriented ceramics using the manufacturing process of

Fig. 5. The effect of tube curvature on the axial (top) and radial (bottom) displacements of the tubes (radial ratio is D/D_h).
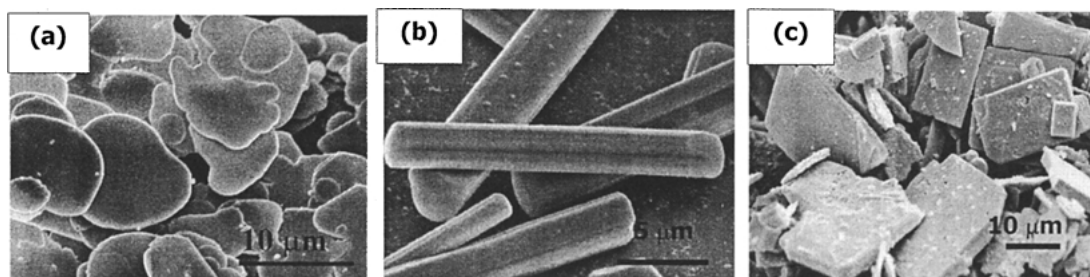
Fig. 6. Anisometric templates for grain-orientation process synthesized by molten salt process: (a) BiT platelets grown at 1150°C, (b) PN needle-like templates grown at 1150°C, and (c) SrTiO₃ tabular templates grown at 1100°C.

FDC. Templates can be oriented during two extrusion steps; first when the filament is extruded and second, when the material is extruded through a fine nozzle during deposition. Three ferroelectric systems of interest, bismuth titanate (BiT, $Bi_4Ti_3O_{12}$), lead metaniobate (PN, $PbNb_2O_6$), and $0.65Pb(Mg_{1/3}Nb_{2/3})O_3$-$0.35PbTiO_3$ (PMN-PT), were investigated.

Bismuth titanate has a high Curie temperature (675°C) [23] and therefore is a candidate for high-temperature piezoelectric devices. Proper poling of random polycrystalline BiT is difficult. It is preferred to have grain-oriented BiT to facilitate and improve poling.

Lead metaniobate ceramics have found applications in acousto-electrics (hydrophones) where a higher d_{33}/d_{31} ratio, and hence, a higher k_t/k_p ratio is beneficial [24]. High d_{33}/d_{31} ratio can be obtained in polycrystalline samples when strong grain orientation is achieved.

PMN-PT single crystals have shown high electromechanical properties in certain crystallographic directions [25, 26]. For example, it is reported that the d_{33} value in the (001) direction is about 2000 pC/N as opposed to 130 pC/N in the (111) direction [27]. Currently, there are many efforts focused on the fabrication of single crystals and grain-oriented polycrystalline PMN-PT. The first step to obtain grain orientation is to synthesize suitable anisometric templates that can be aligned in a shear forming process. We have utilized molten salt synthesis to make anisometric templates for bismuth titanate, lead niobate, and PMN-PT ceramics.

Anisometric Templates for FDC/TGG Technique

In the bismuth titanate system, anisometric BiT templates were synthesized from Bi_2O_3 and TiO_2 in molten "NaCl + KCl" salt at 1150°C for 1 hr (Fig. 6(a)) [28]. The templates were platelet seeds 10–30 μm in diameter and <0.5 μm in thickness, showing aspect ratios of 20–50. In the lead metaniobate system, needle-shaped particles of PN were synthesized from PbO and Nb_2O_5 in molten KCl at 1150°C for 1 h (Fig. 6(b)) [29]. The aspect ratio of the seeds (length to diameter) was estimated to be about ten.

In the PMN-PT system, suitable anisometric templates are not yet manufactured. Several attempts have been made to use other seeds (i.e., heteroepitaxial growth) with suitable structure and lattice parameters. Three families of perovskite templates, namely $PbTiO_3$ ($a_o = 3.90$ Å), $BaTiO_3$ ($a_o = 3.99$ Å) and $SrTiO_3$ ($a_o = 3.90$ Å) are viable candidates for satisfactory lattice/structure matching. Strontium titanate is deemed suitable since anisometric seeds (tabular morphology with high aspect ratio) can readily be synthesized.

Direct synthesis of $SrTiO_3$ results in cubic templates that cannot be aligned in a shear forming process. Therefore, a two-step process was used [30]. First, platelet $Sr_3Ti_2O_7$ particles were synthesized from the desired molar ratio of TiO_2 and $SrCO_3$ powders in molten KCl at 1250°C. The $Sr_3Ti_2O_7$ particles were then reacted with TiO_2 in a second molten salt process at 1100°C to prepare tabular $SrTiO_3$ via epitaxial growth. Figure 6(c) shows tabular seeds with an edge length of about 10–30 μm and thickness of 1–3 μm (aspect ratio ≥ 7).

Grain Oriented Polycrystalline Ceramics

The synthesized anisometric seeds were incorporated into fine matrix powders to make FDC feedstock (filament). About 5–10 vol% templates (relative to

fine polycrystalline powder) was used. During filament preparation, ceramic powder and a thermoplastic binder were extensively mixed (compounded) to uniformly disperse the powder in the binder. This process involved harsh mixing at high shear rates in a torque rheometer. Caution was exercised to avoid damaging the templates during this step. Upon extrusion of the filaments, the orientation status of the templates was investigated. For the platelet BiT or tabular $SrTiO_3$ templates, it was observed that the seeds were aligned on the filament surface, but randomly dispersed within the bulk of the filament. On the other hand, the needle-like PN seeds were oriented properly both on the surface and within the bulk. The geometry (shape and dimensions) of the templates plays a crucial role in the alignment.

Green BiT samples were deposited by FDC and sintered/annealed at 1100°C for 1 hr to induce grain growth and orientation. The X-ray diffraction and microstructure of the sintered samples illustrated partial orientation with a calculated Lotgering [31] factor of 0.46 [28]. These results manifested the potential of using the FDC technique for the development of textured microstructures.

Prototyped PN samples made with seeded PN filaments were sintered at 1100–1300°C for 1 hour. SEM observation of the samples showed elongated grains, mainly aligned parallel to the deposition direction upon sintering at 1250°C (Fig. 7(b)) [29]. This is in contrast to the random polycrystalline microstructure of the pressed sample shown in Fig. 7(a). The XRD results revealed that the PN samples sintered at $T \leq 1250$°C were composed of a mixture of ferroelectric (orthorhombic) and non-ferroelectric (rhombohedral) phases. A fully ferroelectric phase was obtained upon sintering at 1300°C followed by rapid cooling (air quench) to room temperature. Sintered PN samples were poled under an electric field of 20–40 kV/cm

Table 1. Properties of grain-oriented lead metaniobate made by FDC in comparison to pressed (random polycrystalline) samples.

Parameter	Dielectric constant (K)	Charge constant d_{33} (pC/N)	Voltage constant g_{33} (10^3 Vm/N)	Figure of merit $d_{33}g_{33}$ (10^{-15} m^2/N)	Relative density (%)
FDC	210	80	43	3440	84.6
Press	234	65	31	2015	93.1

at 140°C. The measured d_{33} coefficients for grain-oriented samples were ∼80 pC/N. It is anticipated that attainment of higher densities and avoiding microcrack formation upon rapid cooling would result in higher piezoelectric values. Table 1 illustrates other properties of grain-oriented lead metaniobate FDC samples in comparison to pressed samples.

PMN-PT samples were also made with the $SrTiO_3$ seeded filaments. The XRD results indicated improved orientation of the textured PMN-PT samples. In random polycrystalline PMN-PT, the main peak corresponds to the (110) plane at $2\theta \approx 32$° (Fig. 8(a)). However, the diffraction pattern of the textured PMN-PT samples (Fig. 8(b)) exhibits significantly increased (100) and (200) peak intensities. Other peaks including (110) peak are also suppressed relative to the random polycrystalline sample. A d_{33} of about 1100 pC/N was measured upon grain orientation. This is almost twice as much as the value for a random polycrystalline PMN-PT sample. The effect of template volume fraction and other suitable templates (such as barium titanate) are currently being investigated.

Net Shape Single Crystal PMN-PT Components

Recently, a new cost-effective process has been developed to make rather large PMN-PT crystals through
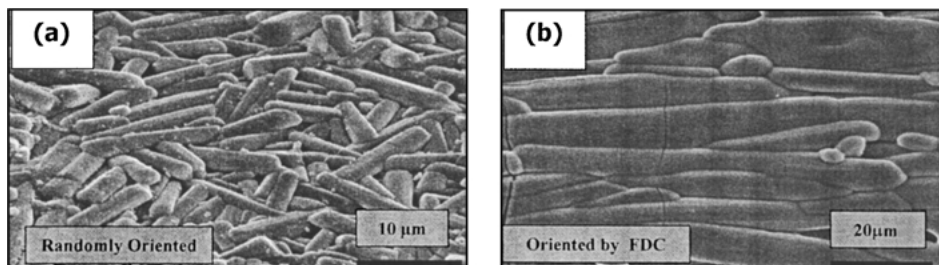

Fig. 7. SEM micrographs of the PN sample (a) pressed sample with random orientation, and (b) grain-oriented microstructure obtained via FDC.
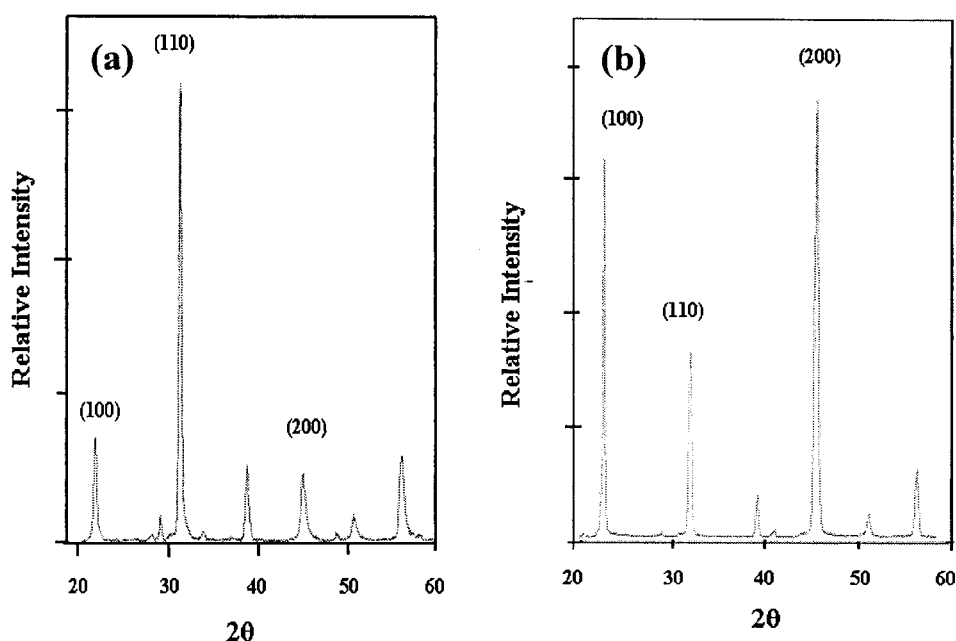
Fig. 8. XRD patterns of 0.65PMN-0.35PT (a) powders and (b) grain-oriented matrix.
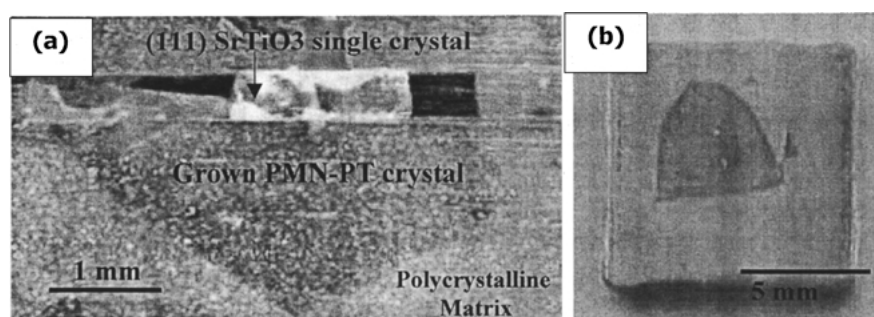

Fig. 9. (a) A photograph of the cross section of the sample illustrating SrTiO$_3$ single crystal, grown single crystal region, and fine polycrystalline matrix upon annealing at 1250°C for 10 hrs. (b) Top view of triangular PMN-PT single crystal grown to the surface of a thin sample.

a conventional powder processing technique, referred to as Seeded Polycrystal Conversion (SPC) [32, 33]. The two methods of TGG and SPC are practically similar with some minor differences. In the SPC process, an embedded seed would induce epitaxial growth into a fine polycrystalline matrix through boundary migration, converting the polycrystalline region into a large single crystal.

We have utilized this technique in combination with FDC to investigate the feasibility of manufacturing net shape single crystal (or single crystal-like) components. In this work, we have used SrTiO$_3$ seeds (5 × 5 × 0.5 mm) and a matrix of fine polycrystalline 0.65PMN-0.35PT with 3 vol% excess PbO. A SrTiO$_3$ single crystal seed was embedded in a polycrystalline matrix halfway through the deposition process. The cross section of the samples, heat-treated at 1250°C for 10 hours, revealed a significant growth of PMN-PT single crystal with a pyramidal shape on top of the (111) SrTiO$_3$ seed (Fig. 9). The maximum growth was approximately 2.5 mm from the surface of the seed to the tip of the pyramid. The grown PMN-PT crystals with (111) and (110) orientations have been cut out of the polycrystalline matrix. The properties of these single crystals are compared with the polycrystalline counterparts upon sintering at 1250°C for 10 hours (Table 2).

Table 2. Comparison of polycrystalline 0.65PMN-0.35PT to single crystal samples with (110) and (111) orientations grown at 1250°C for 10 hours.

Properties	Polycrystalline PMN-PT (65/35)	Single crystal (110)	Single crystal (111)
d_{33} (pC/N)	390	~880	590
Dielectric constant	2650	~4500	~4450
Loss tangent (%)	0.48	0.55	0.33

Although long time treatment at high temperature resulted in property degradation, PMN-PT single crystals show higher d_{33} and dielectric constants than the random polycrystalline PMN-PT.

Currently, spiral and 2-2 structures are deposited on top of SrTiO$_3$ seeds to obtain net shape components with only one single crystal. If successful, this process can be utilized to economically fabricate complex shapes with properties superior to polycrystalline ceramics.

Summary

Rapid prototyping is an efficient tool for design and fabrication of piezoelectric ceramics. It facilitates the process of exploring new designs and characterizing new structures in a rapid, cost-effective manner. The FDC process has been utilized to build several piezoelectric actuators over the last few years. PZT spirals exhibit large field-induced displacements, due to the bending caused by the curved geometry. This effect can be further enhanced by making unimorph spirals (adding stiff metallic shims), and two-materials (piezoelectric/electrostrictive) spirals. The positive effect of curved geometry, demonstrated in spiral and other actuators, was trivial for the axial displacement of the tube actuators with inward and outward curvatures.

Net shape grain oriented ceramics of bismuth titanate, lead metaniobate, and PMN-PT ceramics were fabricated using anisometric (platelet and needle-like) templates aligned in fine powder matrices. Strong orientation was observed in lead metaniobate samples upon sintering/annealing at 1300°C whereas only partial orientation was seen in bismuth titanate. It appears that needle-like templates can be aligned much more efficiently than the platelet templates during the fused deposition process. Grain-oriented 0.65PMN-0.35PT ceramics were also manufactured using tabular SrTiO$_3$ seeds. Although partial grain orientation was achieved upon sintering, a significant improvement was observed in the electromechanical properties of the textured samples. This was achieved due to the proper orientation of the PMN-PT sample in the (001) direction. Single crystals of PMN-PT were also grown at 1250°C using embedded (111) and (110) SrTiO$_3$ seeds. The feasibility of making net shape single crystal PMN-PT components is currently being examined.

Acknowledgments

References

1. G.H. Haertling, *Am. Ceram. Soc. Bull.*, **73**, 93 (1994).
2. F. Mohammadi, A. Kholkin, B. Jadidian, and A. Safari, *Applied Physics Letters*, **75**, 2488 (1999).
3. Q.M. Wang, Q. Zhang, B. Xu, R. Liu, and L.E. Cross, *Journal of Applied Physics*, **86**, 3352 (1999).
4. A. Safari, S.C. Danforth, M.A. Jafari, M. Allahverdi, B. Jadidian, F. Mohammadi, N. Vankataraman, and S. Rangarajan, in *Proceedings of the 9th European Conference on Rapid Prototyping and Manufacturing*, edited by R.I. Campbell (University of Nottingham, Nottingham, UK, 2000), p. 247.
5. A. Safari and S.C. Danforth, in *Proceedings of the 11th IEEE International Symposium on the Applications of Ferroelectrics*, edited by E. Colla, D. Damjanovic, and N. Setter, (IEEE-UFFC, New Jersey, 1998), p. 229.
6. A. Bandyopadhyay, R.K. Panda, T.F. McNulty, F. Mohammadi, S.C. Danforth, and A. Safari, *Rapid Prototyping Journal*, **4**, 37 (1998).
7. A. Safari and M. Allahverdi, *Ceram. Eng. Sci. Proc.*, **22**, 473 (2001).
8. F. Mohammadi, Ph.D. Thesis, Department of Ceramic and Materials Engineering, Rutgers University, New Jersey, USA (2001).
9. F. Mohammadi, A. Kholkin, S.C. Danforth, and A. Safari, in *Proceedings of the 11th IEEE International Symposium on the Applications of Ferroelectrics*, edited by E. Colla, D. Damjanovic, and N. Setter (IEEE-UFFC, New Jersey, 1998), p. 273.
10. S.A. Wise, *Sensors and Actuators* A, **69**, 33 (1998).
11. Q. M. Zhang, H. Wang, and L.E. Cross, *J. Mater. Sci.*, **28**, 3962 (1993).
12. Y. Sugawara, K. Onitsuka, S. Yoshikawa, Q.C. Xu, R.E. Newnham, and K. Uchino, *J. Am. Ceram. Soc.*, **75**, 996 (1992).
13. A.M. Umarji, A.L. Kholkin, T.F. McNulty, S.C. Danforth, and A. Safari, in *Proceedings of the 11th IEEE International Symposium on the Applications of Ferroelectrics*, edited by E. Colla, D. Damjanovic, and N. Setter (IEEE-UFFC, New Jersey, 1998), p. 269.

14. T.W. Chou, B.A. Cheeseman, A. Safari, and S.C. Danforth, *Ceramic Eng. Sci. Proc.*, **22**, 497 (2001).

15. Q.M. Zhang, H. Wang, and L.E. Cross, *J. Mater. Sci.*, **28**, 3962 (1993).

16. J. Chen, Q.M. Zhang, L.E. Cross, and C.M. Trottier, in *Proceedings of International Conference on Intelligent Materials (ICIM) 1994*, 5–8 June 1994, Williamsburg, VA, p. 316.

17. M. Allahverdi and A. Safari, *J. Eur. Ceram. Soc.*, **21**, 1485 (2001).

18. M. Allahverdi, B. Jadidian, B. Harper, S. Rangarajan, M. Jafari, S.C. Danforth, and A. Safari, in *Proceedings of 12th IEEE International Symposium on Applications of Ferroelectrics*, edited by S.K. Streiffer, B.J. Gibbons, and T. Tsurumi, (IEEE-UFFC, New Jersey, 2001), p. 381.

19. J.A. Horn, S.C. Zhang, U. Selvaraj, G.L. Messing, and S. Trolier-McKinstry, *J. Am. Ceram. Soc.*, **82**, 921 (1999).

20. M. Holmes, R.E. Newnham, and L.E. Cross, *Am. Ceram. Soc. Bull.*, **58**, 872 (1979).

21. M.M. Seabaugh, I.H. Kerscht, and G.L. Messing, *J. Am. Ceram. Soc.*, **80**, 1181 (1997).

22. P.W. Rehrig, G.L. Messing, and S. Trolier-McKinstry, *J. Am. Ceram. Soc.*, **83**, 2654 (2000).

23. A. Fouskova and L.E. Cross, *J. Appl. Phys.*, **41**, 2834 (1970).

24. P. Eyraud, L. Eyraud, P. Gonnard, D. Noterman, and M. Troccaz, in *Proceedings of 6th IEEE International Symposium on Applications of Ferroelectrics*, edited by B.M. Kulwicki, A. Amin, and A. Safari (IEEE-UFFC, New Jersey, 1996), p. 410.

25. S.-E. Park and T.R. Shrout, *J. Appl. Phys.*, **82**, 1804 (1997).

26. S.-E. Park and T.R. Shrout, *Mater. Res. Innovations*, **1**, 20 (1997).

27. G. Xu, H. Luo, Y. Guo, Y. Gao, H. Xu, Z. Qi, W. Zhong, and Z. Yin, *Solid State Communications*, **120**, 321 (2001).

28. M. Allahverdi, B. Jadidian, Y. Ito, and A. Safari, in *Proceedings of 12th IEEE International Symposium on Applications of Ferroelectrics*, edited by S.K. Streiffer, B.J. Gibbons, and T. Tsurumi (IEEE-UFFC, New Jersey, 2001), p. 385.

29. K. Nonaka, M. Allahverdi, and A. Safari, in *Innovative Processing and Synthesis of Ceramics, Glasses, and Composites V*, Ceramic Transactions, Vol. 129, 199 (2002).

30. K. Watari, B. Brahmaroutu, G.L. Messing, S. Trolier-McKinstry, and S.C. Cheng, *J. Mater. Res.*, **15**, 846 (2000).

31. F.K. Lotgering, *J. Appl. Phys.*, **39**, 2268 (1968).

32. A. Khan, F.A. Meschke, T. Lao, A.M. Scotch, H.M. Chan, and M.P. Harmer, *J. Am. Ceram. Soc.*, **82**, 2958 (1999).

33. T. Li, S. Wu, A. Khan, A.M. Scotch, H.M. Chan, and M.P. Harmer, *J. Mater. Res.*, **8**, 3189 (1999).